Structure and Interaction of PA63 and EF (Edema Toxin) of *Bacillus anthracis* with Lipid Membrane†

Xiao-Ming Wang,‡ Ruddy Wattiez,§ Michèle Mock,⊥ Paul Falmagne,§ Jean-Marie Ruysschaert,‡ and Véronique Cabiaux*,‡

Laboratoire de Chimie Physique des Macromolécules aux Interfaces, CP 206/2, Université Libre de Bruxelles, Boulevard du Triomphe, 1050 Brussels, Belgium, Service de Chimie Biologique, Université de Mons-Hainaut, Avenue Maistriau 21, 7000 Mons, Belgium, and Laboratoire de Génétique Moléculaire des Toxines (URA 1858, CNRS), Institut Pasteur, 28 Rue du Docteur Roux, 75724 Paris Cedex 15, France

Received July 9, 1997⊗

ABSTRACT: The secondary structures of the two components of the *Bacillus anthracis* edema toxin, protective antigen (PA63) and edema factor (EF), as well as the two EF mutants: CYA30 (containing the N-terminal PA63-binding domain) and CYA62 (containing the C-terminal catalytic domain) were investigated as a function of pH in the absence and in the presence of phospholipid vesicles using attenuated total reflection Fourier transform infrared spectroscopy. Secondary structures were independent of pH, whereas, in all cases, structural modifications were observed upon lipid binding. The ability of PA63 and EF to undergo hydrogen/deuterium exchange was evaluated. The binding of these proteins and the mutants to the lipid membrane was also characterized and it was demonstrated that the association of PA63 to the lipid bilayer was pH-dependent, while the binding of EF to the lipid membrane took place at both neutral and acidic pH. Interestingly, the two EF mutants are showing different lipid binding properties in response to pH: CYA30 has a strong pH-dependence whereas CYA62, as EF, binds to the lipid vesicles at all pHs. For the two proteins characterized by a pH-dependent lipid binding, the reversibility of binding upon neutralization was tested and binding of PA63 to the membrane was found to be irreversible whereas that of CYA30 was reversible.

The two toxins produced by the bacterium *Bacillus anthracis* (*1*) are included in a group of bipartite, bacterial protein toxins that are organized structurally into distinct effector (A) and receptor-binding (B) domains. The anthrax toxins differ from the prototypical diphtheria toxin, however, since a single B domain, protective antigen (PA, 83 kDa), interacts separately with two A domains, edema factor (EF, 89 kDa) and lethal factor (LF, 83 kDa),[1] to produce biologically distinct effects: the PA−LF complex, designated as lethal toxin, leads to death in rats and other animals (*2*) whereas the PA−EF complex, designated as edema toxin, causes edema when injected intradermally (*3*).

According to the proposed pathways of EF and LF intoxication (*1*), PA binds to a specific cell surface receptor of approximately 85−90 kDa, as identified on CHO-K1 cells (*4*). The bound PA is then proteolytically nicked (*5*), probably by furin (*6, 7*). This cleavage generates two fragments of which the small one (PA 20, M_r 20 kDa) is released in the outside medium and the larger one (PA63, M_r 63 kDa), remains attached to the receptor. A newly exposed site on PA63 allows the binding of EF or LF, which, otherwise, cannot bind to the cell surface (*8*). After either EF or LF binding to PA63, the receptor−PA63−LF (or EF) complex is endocytosed by receptor-mediated endocytosis. As previously demonstrated for diphtheria toxin (DT) (*9, 10*), an acidic pH is crucial for intoxication, since the cells are completely protected from *B. anthracis* edema toxin and lethal toxin by pretreatment with ammonium chloride and chloroquine, which dissipate the intracellular proton gradients and raise the pH of intracellular vesicles (*11, 12*). Both EF and LF are thought to act on intracellular targets. EF has been shown to be a calcium- and calmodulin-dependent adenylate cyclase, which causes a dramatic elevation of cAMP within cells (*13*−*15*). Recent evidences that protease inhibitors prevent the intoxication of macrophages by lethal toxin and that LF is fully inactivated by mutagenesis of a zinc-binding site suggest that LF is a Zn-metalloprotease (*16*) whose target still remains to be identified.

In a previous paper, we investigated the effect of pH upon PA (the full-length protein) and LF binding to lipids, and we have characterized the secondary and tertiary structures of PA and LF as a function of pH and the presence or the absence of lipid vesicles (*17*). However, even though PA

† X.M.W. is an ARC (Actions de Recherches Concertées, Belgium) fellow. V.C. is research associate of the National Fund for Scientific Research (Belgium).

* To whom correspondence should be addressed. Tel: +32 2 650 5365. Fax: +32 2 650 5113. E-mail: vcabiaux@ulb.ac.be.

‡ Université Libre de Bruxelles.

§ Université de Mons-Hainaut.

⊥ Institut Pasteur.

⊗ Abstract published in *Advance ACS Abstracts,* November 15, 1997.

[1] Abbreviations: ATR-FTIR, attenuated total reflection Fourier transform infrared spectroscopy; CYA30, deletion mutant of the adenylate cyclase of *B. anthracis*, containing the N-terminal 303 residues; CYA62, deletion mutant of the adenylate cyclase of *B. anthracis*, lacking the N-terminal 261 residues; EF, edema factor; LF, lethal factor; PA, protective antigen; PA20, the N-terminal 20 kDa of protective antigen; PA63, the C-terminal 63 kDa of protective antigen; DT, diphtheria toxin; Hepes, 4-(2-hydroxyethyl)-1-piperazineethanesulfonic acid; LUV, large unilamellar vesicles; SDS−PAGE, sodium dodecyl sulfate polyacrylamide gel electrophoresis; PMSF, phenylmethylsulfonyl fluoride; PVDF, polyvinylidene difluoride; Tris, 2-amino-2-(hydroxymethyl)-1,3-propanediol.

S0006-2960(97)01661-9 CCC: $14.00

can insert in a lipid membrane (*18*), the cell membrane active form is PA63 which has been demonstrated to form cation-selective channels in planar phospholipid bilayers (*19*), and to induce the release of markers from vesicles and cells at acidic pH (*20*−*22*). To provide information about the mechanism of insertion of PA63 in the lipid membrane, we have characterized the lipid binding of PA63 and its structure as a function of pH and the presence or the absence of a lipid bilayer. A similar study was carried out with EF and two of its mutants: CYA30, which contains the N-terminal PA63-binding domain, and CYA62, which carries the binding sites required to express the catalytic activity (*15*). The obtained data are discussed in terms of the intoxication pathway of the two toxins of *B. anthracis*.

MATERIALS AND METHODS

Materials. Trypsin, soybean trypsin inhibitor, and asolectin (mixed soybean phospholipids) were obtained from Sigma Chemical Co. (St. Louis, MO). Asolectin was purified according to the method of Kagawa and Racker (*23*). D_2O was from Merck (Germany). Acrylamide and Coomassie Blue R-250 were from Bio-Rad. All other reagents were of the highest purity available.

Purification of PA63, EF, CYA30, and CYA62. The anthrax edema toxin proteins (PA and EF) were produced by double mutant strains of *B. anthracis*, in which two of the three toxin genes (*lef*, *cya*, and *pag*) were respectively inactivated by intragenic deletion (*lef*,*cya* or *lef*,*pag*). These strains were capable of producing only a single toxin component and were used to avoid the possible contamination from the two other proteins (*24*). The culture and purification of PA and EF were carried out as previously described (*24*). PA63 was generated by "nicking" PA with trypsin (trypsin/PA, 1/100, w/w) in a 20 mM Tris-HCl buffer, pH 7.2, for 15 min at 30 °C. The reaction was stopped by the addition of soybean trypsin inhibitor (trypsin/inhibitor, 1/10, w/w) and of 2 mM PMSF. The sample was subsequently purified by chromatography on a Mono-Q HR 5/5 anion-exchange column (Pharmacia, Uppsala, Sweden) using a 20 mM ethanolamine buffer, pH 9.0, and a 0−450 mM NaCl gradient. The purity of PA63 and EF was over 95% as judged by 12% SDS−PAGE stained with Coomassie Blue R-250 (*25*). For the FTIR experiments, the proteins were dialyzed against a 2 mM Hepes buffer, pH 7.2, overnight and stored at −20 °C.

CYA30 (N-terminal 303 residues) and CYA62 (C-terminal 539 residues) are two mutants of the EF protein. CYA62 is the product of the plasmid pMMA861.19N in which the first 261 codons of the *cya* gene were removed (*15*). The protein was purified according to Labruyère et al. (*15*), and the lyophilized sample was resuspended in a 2 mM Hepes buffer, pH 7.3. CYA30 is the product of the plasmid pMMA111 which harbors a deletion of the *cya* gene preserving the 303 codons at the 5′-end. This plasmid was introduced in the *pag* and *lef* mutant of *B. anthracis*, which produces only EF. This strain secretes CYA30 with only a minor contamination due to EF. To remove the full-length protein, we made use of the strong affinity of EF for calmodulin. The culture supernatant was incubated with a calmodulin-Sepharose resin (Pharmacia) in a 50 mM Tris buffer, pH 7.4, 2 mM $CaCl_2$, at room temperature for 1 h under shaking. The mixture was packed in a 10 mL column, and the liquid flowing through the column was recovered. To increase the yield of recovery, the column was washed with 1 mL of the same buffer. The overall process was repeated four times. The eluant which contains CYA30 was eventually dialyzed against a 20 mM Tris buffer, pH 8.0, and purified on the Mono-Q column using the dialyzing buffer and a 0−400 mM NaCl gradient.

Amino Acid Microsequence Analysis. Sample proteins were separated by SDS−PAGE and electroblotted onto polyvinylidene difluoride (PVDF) membranes as described by Matsudaira (*26*). The blot was stained with Coomassie Blue. Amino acid microsequence analysis of the electroblotted proteins was performed by automated Edman degradation of 1−10 pmol of protein on a Beckman LF3400 protein−peptide microsequencer equipped with an on-line Gold 126 microgradient high-pressure liquid chromatography system and a Beckman Instruments, Inc., model 168 diode array detector (Fullerton, CA). All samples were sequenced using standard Beckman Sequencer Procedure 4. Alkylation of cysteine with acrylamide for sequencing was performed "*in situ*" as described by Brune (*27*). The phenylthiohydantoin amino acid derivatives were quantitatively identified by reverse phase high-pressure liquid chromatography on an ODS Spherogel micro phenylthiohydantoin column (3 μm diameter particles, 2 × 150 mm, Beckman Instruments). All sequencing reagents were from Beckman.

Liposome Preparation. Asolectin was kept as a stock solution in chloroform (100 mg/mL). A film of asolectin was formed on a glass tube and dried overnight under vacuum. This film was rehydrated in a 10 mM Hepes buffer, pH 7.2, 150 mM NaCl. Large unilamellar vesicles (LUV) were formed by an extrusion procedure (pores: 0.1 μm diameter) at room temperature according to Hope et al. (*28*). The concentration of lipids was determined by measuring the lipid phosphorus content (*29*).

Association to Lipid of PA63, EF, CYA30, and CYA62. Forty micrograms of PA was mixed with 300 μg of LUV in a 20 mM Tris buffer, pH 7.2, and incubated 10 min at 37 °C. The system was treated with trypsin (trypsin/PA, 1/100, w/w) for 15 min at 30 °C. The reaction was blocked by addition of soybean trypsin inhibitor (trypsin/inhibitor, 1/10, w/w). The pH was then lowered to the desired one by addition of a predetermined volume of 1 M sodium acetate, pH 5.0. After 10 min of incubation at 37 °C, the samples were then mixed with an equal volume of 80% sucrose and overlaid with a 30−2% linear sucrose gradient. For EF, CYA30, and CYA62, 40 μg of proteins and 300 μg of LUV were mixed at pH 7.2 and incubated for 10 min at 37 °C. After adjustment to the desired pH and incubation for 10 min at 37 °C, the samples were submitted to a sucrose gradient as described above. After an overnight centrifugation at 125000*g* at 4 °C in a Beckman L7 ultracentrifuge with a SW60 rotor, the gradients were fractionated from the bottom to the top of the tube, and the phospholipid and protein distributions were determined respectively by a choline dosage (test combination phospholipids, Boehringer Mannheim Biochemia) and by measuring the Trp fluorescence (λ_{ex} = 280 nm and λ_{em} = 340 nm) or the Tyr fluorescence (λ_{ex} = 277 nm and λ_{em} = 303 nm) using a JY3D (Jobin Yvon) spectrofluorometer. As Tyr fluorescence is much weaker than Trp fluorescence, the absorption of the sucrose was subtracted from the signal. Fractions which contained both lipids and proteins were pooled, centrifuged,

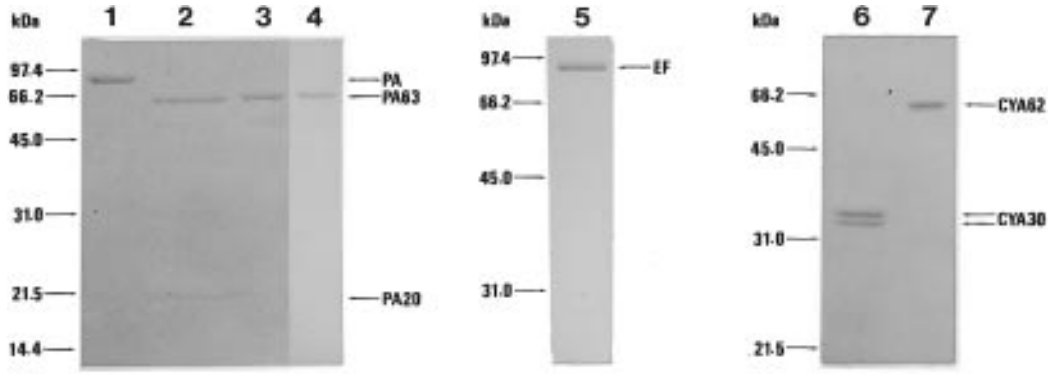

FIGURE 1: (Lanes 1−4) 12% SDS−PAGE (1) PA, (2) nicked PA (in the presence of the vesicles and before the sucrose gradient), (3) lipid-bound PA63, and (4) purified PA63. (Lanes 5−7) 10% SDS−PAGE (5) EF, (6) CYA30, and (7) CYA62.

and washed twice with a 2 mM Hepes buffer at desired pH to remove the sucrose. To study the reversibility of the association of the proteins showing a pH-dependent lipid binding, the lipid-bound protein samples were divided in two parts: one half was kept at low pH and the other half was brought back to pH 7.2 by addition of a predetermined volume of 1 mM NaOH. The two samples were then submitted to a sucrose gradient as described above.

IR Spectroscopy. Attenuated total reflection infrared spectra (resolution of 4 cm^{-1}) were obtained on a Perkin-Elmer 1720X FTIR spectrophotometer as previously described (*30*). Measurements were carried out at room temperature. Thin films were obtained by slowly evaporating a sample under a stream of nitrogen on one side of the ATR plate (Germanium plate) (*31, 32*). The ATR plate was then sealed in a universal sample holder (Perkin-Elmer 186-0354) and deuterated by flushing the sample compartment with D_2O-saturated N_2 at room temperature for 90 min. The hydrogen/deuterium exchange allows differentiation of the α-helix from the random structure, whose absorbance band shifts from about 1655 cm^{-1} to about 1642 cm^{-1} (*33, 34*). The determination of the secondary structure of proteins was carried out by analysis of the deuterated amide I region as described previously (*30, 35*−*37*). The frequency limits for the different structures were as follows: 1662−1645 cm^{-1}, α-helix; 1689−1682 cm^{-1} and 1637−1613 cm^{-1}, *β*-sheet; 1645−1637 cm^{-1}, random coil; and 1682−1662 cm^{-1}, *β*-turns. The control spectra of the 2 mM Hepes buffer, pH 7.2, and asolectin vesicles at both pH 7.2 and 5.0 showed no absorbance between 1700 and 1600 cm^{-1} (data not shown).

Kinetics of Deuteration. The experimental procedure was carried out as previously described (*17, 30*). The pH of each sample was checked to ensure that it was either 7.2 or 5.0. If it was not, the pH was adjusted with diluted HCl or NaOH. The samples were spread on a germanium plate as described above (*31, 32*). At time zero, a D_2O saturated N_2 flux was applied to the sample, with a flow rate of 75 mL/min controlled with a Brooks flowmeter. The spectra at each time point were the accumulation of 12 scans with a resolution of 4 cm^{-1}. The background due to the atmospheric water contribution was computed as described in Goormaghtigh et al. (*30*) and was subtracted from each spectrum. The amide I and II band areas were measured between 1702−1596 and 1585−1502 cm^{-1}, respectively. The amide II area was divided by the amide I area for each spectrum to take into account any change in the total intensity of the spectra during the deuteration process. This ratio, which was expressed between 0 and 100%, was plotted versus deuteration time. The 100% value is defined by the amide II/amide I ratio obtained before deuteration, whereas the 0% value corresponds to a zero absorbance in the amide II region. It has been shown previously (*38, 39*) on a series of proteins which can be fully denatured (and therefore fully deuterated in the denatured state) and then refolded to their original structure, that complete H/D exchange resulted in 0 + 5% absorbance in the amide II region. We are therefore confident that a zero absorbance in the amide II region reflects the full deuteration of the protein.

RESULTS

Purification of Soluble PA63, Lipid-Associated PA63, EF, and the Two Mutants of EF. Soluble PA63 was generated by "nicking" PA with trypsin and purified by chromatography of trypsin-treated PA on a Mono-Q anion-exchange resin using a pH 9.0 ethanolamine buffer and a 0−450 mM NaCl gradient as described under Materials and Methods. PA63 was eluted at about 380 mM of NaCl in a single peak (data not shown). The fractions corresponding to the peak were collected, and figure 1 (lane 4) shows that they contained a single band with an apparent molecular mass of 63 kDa. However, the yield of the purification was quite low since PA63 has a strong tendency to aggregate as the sample is aging. Therefore, this method of purification was used only to generate the lipid-free and soluble form of PA63, which was devoted to the FTIR study, and another method was developed to prepare and to insert PA63 in the lipid membrane by a single step. The incubation of PA with trypsin was carried out at pH 7.2 in the presence of asolectin large unilamellar vesicles, the pH was dropped to 5.0, and the sample was run on a sucrose gradient to remove the non-associated proteins. Figure 1 shows that before the sucrose gradient (lane 2), both PA63 and PA20 were present in the sample whereas, after purification of the protein-bound lipid (lane 3), only PA63 was identified. The N-terminal sequence of this protein was determined and was shown to correspond to the expected trypsin cleavage site between R^{167} and S^{168}. This suggests that carrying the "nicking" in the presence of the lipid vesicles followed by the pH drop is a straightforward and efficient method to obtain PA63 in a lipid environment.

The Coomassie Blue-stained SDS−PAGE gel also shows that the EF (Figure 1, lane 5) and CYA62 (Figure 1, lane 7) samples contained a single band at about 89 kDa and 62 kDa, respectively. On the contrary, two bands were identified in the CYA30 sample (Figure 1, lane 6). The N-terminal

sequence of these two bands were found to be -[6]TES-DIKRNHKTEKN and -[13]NHKTEKNKTEKEKF. These two bands have been repeatedly identified in several preparations (E. Labruyère, personal communication), suggesting that some proteolysis may take place during protein expression and purification. This sample was used without further purification.

The two toxins of *B. anthracis*, lethal toxin (PA and LF) and edema toxin (PA and EF), have been proposed to enter the cells through receptor-mediated endocytosis. Moreover, the activities of these toxins are blocked by incubation of the cells with drugs known to increase the low intracellular pH, therefore suggesting the involvement of an acidic organelle in the toxin-mediated cytotoxicity (*11*, *12*). We have therefore characterized the effect of pH on both the association of PA63 (the nicked and translocation-active form of PA; *22*), EF, CYA30, and CYA62 to lipid vesicles and their structures in the absence or the presence of lipid vesicles.

Effect of pH upon PA63, EF, CYA30, and CYA62 Association to Liposomes. PA63 and EF were associated to the lipid vesicles at pH 7.2 and 5.0, and the samples were centrifuged on a sucrose gradient as described under Materials and Methods. The sucrose gradients were fractionated, and the proportions of proteins and lipids were determined in each fraction (Figure 2). The association of PA63 to the lipid membrane is pH-dependent (Figure 2, A1 and A2) whereas EF shows a similar efficiency to interact with the lipid membrane at pH 7.2 and 5.0, 100% of the protein being lipid-associated at both pH (Figure 2, B1 and B2). The high protein signal observed at the bottom of the gradient in the PA63 experiments was mostly due to the presence of the trypsin, the trypsin inhibitor, and PA20 (see Materials and Methods for the preparation of that sample). Therefore, to further characterize the pH-dependence of PA63−lipid binding, the proportion of lipid-bound PA63 as a function of pH was determined after fractionation of the sample by a sucrose gradient using a calibration curve built by FTIR as described in Wang et al. (*17*). Briefly, increasing quantities of a protein (LF) were mixed with a fixed quantity of asolectin LUV, and the FTIR spectra of the samples were recorded. The calibration curve was established by plotting log[area amide I/area ν(C═O) lipid] versus log (protein/lipid, w/w). The fractions of the sucrose gradient containing the lipid-bound PA63 were then analyzed by FTIR. The protein/lipid ratio in these samples was determined by measuring the area amide I/area ν(C═O) lipid and by reporting this value on the calibration curve. Binding of PA63 to the lipid vesicles shows a very sharp pH-dependence with a transition pH (pH at which 50% of the protein is associated) at about 5.6−5.7 (Figure 2C). By analogy with full-length PA which has been shown to be irreversibly bound to the membrane when the pH was brought back to neutral (*17*), the reversibility of the lipid binding of PA63 was also studied. A suspension of lipid-bound PA63 at pH 5.0 was divided in two parts: one half was kept at pH 5.0 and the other half was brought back to pH 7.2. The two samples were then run on a sucrose gradient, and the percentage of lipid-bound protein was determined by FTIR, as described above. Reversal of the pH had no effect on the percentage of PA63 bound to the lipid membrane (data not shown), suggesting the irreversibility of its binding.

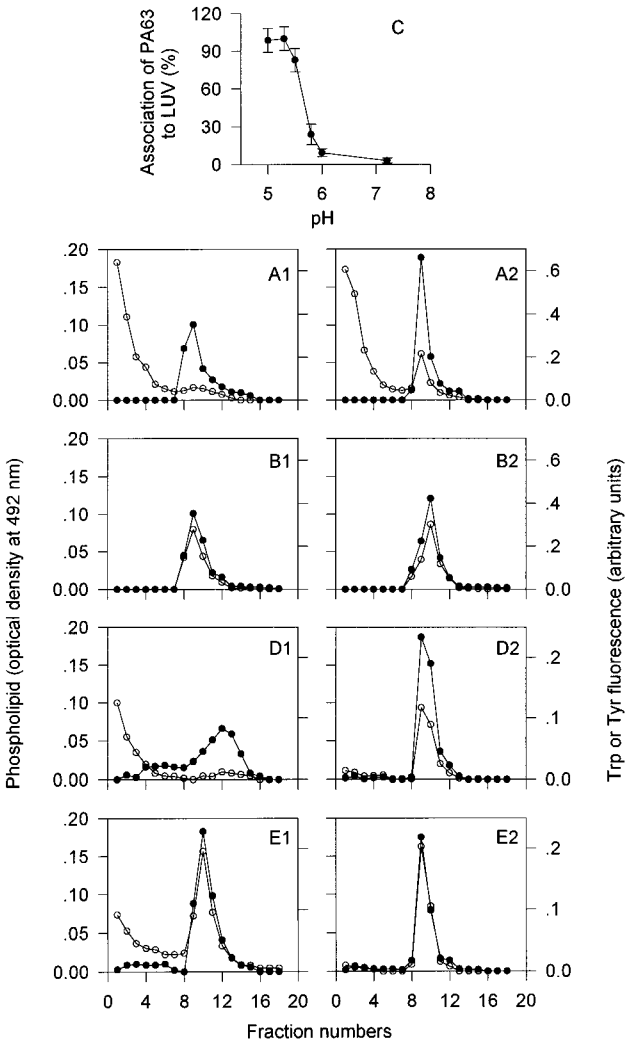

FIGURE 2: Sucrose gradient profiles of PA63 (A), EF (B), CYA30 (D), and CYA62 (E) incubated with liposomes at pH 7.2 (1) and pH 5.0 (2). Eighteen fractions were collected from the bottom to the top of the sucrose gradient and measured for protein (○) and lipid (●) contents. (C) association of PA63 to liposomes as a function of pH. The association was expressed in percentage, in which the maximum protein/lipid ratio (see Materials and Methods) was considered as 100%. The error bars give the standard deviation (three independent experiments).

To further characterize the association of EF to the lipid vesicles, the two truncated mutants (CYA30 and CYA62) were associated to the lipid vesicles at pH 7.2 and 5.0, as described above. Interestingly, the association of CYA30 to the lipid membrane is pH-dependent with virtually no association at pH 7.2 (Figure 2, D1 and D2), while that of CYA62 shows only a slight pH-dependence, 80% and 100% of the protein being membrane-bound at pH 7.2 and 5.0, respectively (Figure 2, E1 and E2) (determined by FTIR as described above). The association of CYA30 to the lipid membrane was fully reversible when the pH was brought back to neutral, as described under Materials and Methods (data not shown).

Effect of pH and the Presence of Lipids on the Structure of Anthrax Edema Toxin Proteins. Investigation of the effect of pH and the presence of a lipid membrane upon toxin structure should provide important information for the understanding of the *B. anthracis* toxin's molecular mechanism of intoxication. The Fourier transform infrared spectroscopy is based on the analysis of the vibration bands

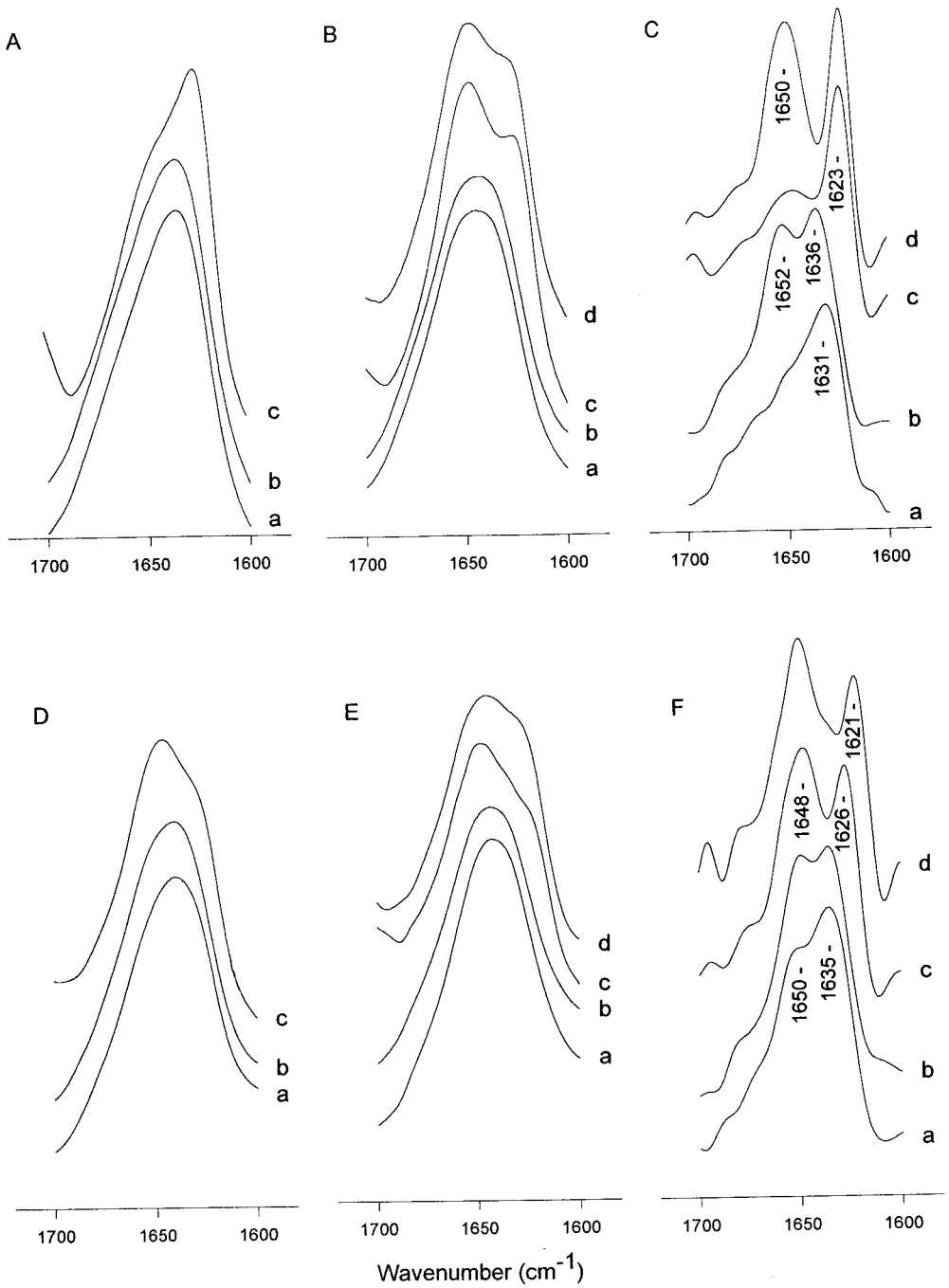

FIGURE 3: Deuterated infrared spectra of PA63 (A), EF (B), CYA30 (D), and CYA62 (E) as a function of pH and the presence of the lipid membrane. Each sample was incubated for 30 min at the desired pH before being spread at the surface of a germanium plate. (a) pH 7.2; (b) pH 5.0; (c) in asolectin LUV at pH 5.0; and (d) in asolectin LUV at pH 7.2. Deconvolved IR spectra (resolution factor, $k = 2$) of PA63 and EF (C) and CYA30 and CYA62 (F) at pH 5.0 without (a, b) and with (c, d) asolectin LUV, respectively.

of protein and particularly the amide I band, ν(C═O) of the peptidic bond, whose frequency of absorbance is strongly dependent upon the secondary structure. This method has been successfully used to investigate the structure of soluble and membrane proteins (*17, 32, 35, 37, 40*−*45*).

The FTIR spectra of chromatography-purified PA63 (A) and of EF (B) at pH 7.2 and 5.0 are shown Figure 3. The secondary structures of PA63 and EF are independent of pH and characterized by maxima of absorbance at 1631, 1652, and 1636 cm^{-1}, respectively (Figure 3C). The absorbance in the 1631 cm^{-1} region characterizes the presence of β-sheet structure, whereas the absorbance at 1652 cm^{-1} indicates the presence of α-helical structure. Table 1 gives the secondary structure contents of PA63 and EF. Incubation of PA63 at pH 5.0 and of EF at pH 7.2 and 5.0 with asolectin LUV results in a slight increase of the helical content (Figure 3

Table 1: Percentage of Secondary Structures (±5%; *35*) of PA63, EF, CYA30, and CYA62 at pH 5.0 in the Absence or Presence of Asolectin LUV

	α-helix (%)	β-sheet (%)	random (%)	turns (%)
PA63	23	34	14	29
PA63 + LUV	34	38	10	18
EF	39	28	15	18
EF + LUV	47	27	7	19
CYA30	27	31	16	26
CYA30 + LUV	39	29	17	15
CYA62	28	31	17	24
CYA62 + LUV	34	31	19	16

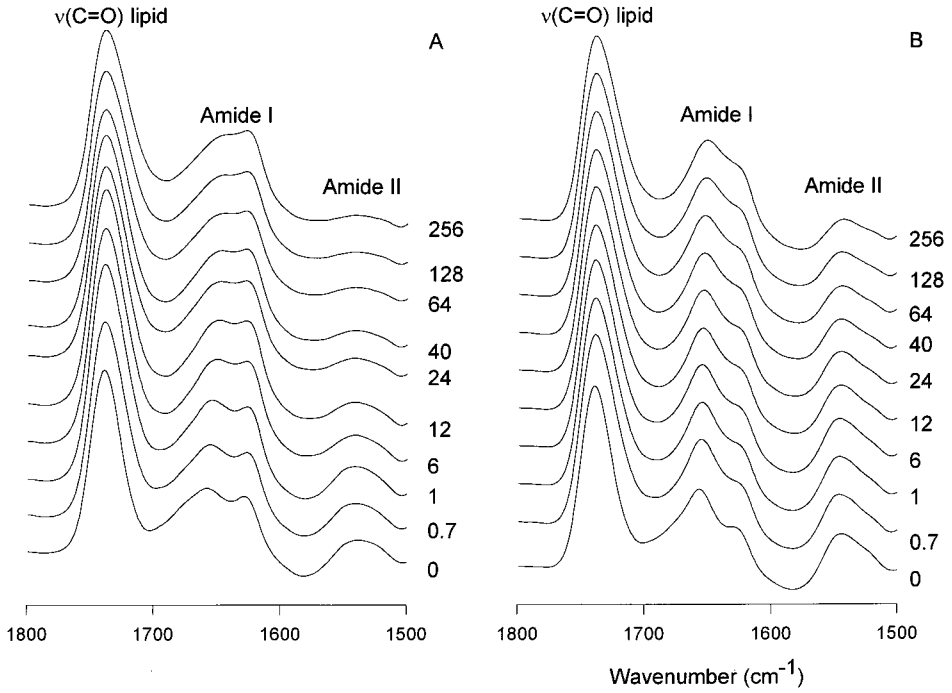

FIGURE 4: IR spectra between 1800 and 1500 cm^{-1} of lipid-bound PA63 (A) and EF (B) at pH 5.0. Spectra were recorded as a function of time of exposure to D_2O-saturated N_2 flow, which is indicated at the right side of the figure. Each group of kinetics spectra is from one of three independent experiments.

and Table 1), whereas the β-sheet content is not modified. However, in both cases, the β-sheet structure, characterized by a maximum of absorption at 1631 (PA63) and 1636 cm^{-1} (EF) in the absence of lipids, is shifted to 1623 cm^{-1} in the presence of the lipid vesicles (Figure 3C). This suggests that the nature of the hydrogen bonds between the sheets is modified upon interaction with the lipid membrane.

The secondary structures of CYA30 and CYA62 are independent of pH (pH 7.2 and 5.0, Figure 3, D and E) with maxima of absorbance at 1650 and 1635 cm^{-1} for CYA30 and 1648 and 1635 cm^{-1} for CYA62 (Figure 3F). In the presence of asolectin LUV at pH 5.0, in both cases, the 1635 cm^{-1} component is shifted to lower wavelength (1626 or 1621 cm^{-1}, Figure 3F), and the α-helical content of the proteins is increased (Table 1).

To further characterize the conformational changes taking place upon lipid binding, the kinetics of deuteration of PA63 and EF in the presence or the absence of the lipid membrane at pH 5.0 and at pH 7.2 and 5.0, respectively, were measured. Indeed, the rate of H/D exchange is related to the solvent accessibility of the NH amide groups of the protein. Peptide hydrogen exchange of the proteins was followed by monitoring the amide II absorbance peak [δ(N−H) maximum in the 1596−1502 cm^{-1} region] decreases because of its shift to the 1460 cm^{-1} region [amide II′, δ(N−D)] upon deuteration (Figure 4). As an example, Figure 4 shows the kinetics of deuteration of PA63 and EF at pH 5.0 in the presence of the lipid membrane. The percentages of non-exchanged residues, calculated from the ratio of amide II/amide I as described under Materials and Methods, are given, in all cases, in Figure 5. At pH 5.0, PA63 is undergoing a fast and extensive exchange: only 25−30% of the residues remained unexchanged after 4 h of deuteration, suggesting that most of PA63 is accessible to solvent. At pH 7.2 and 5.0, 40% of EF residues are resistant to hydrogen/deuterium exchange, which suggests that EF in solution might have a more compact shape than PA63. In any case, the proportion of non-exchanged residues is not significantly modified by the interaction with the lipid membrane, which suggests either that a very low number of residues are protected by the lipid membrane, in addition to those which are buried in the protein, or that a similar number of residues that are protected in the free protein because of the folding are now protected from the solvent because of their insertion in the lipid membrane.

DISCUSSION

The mechanism by which bacterial toxins cross their target membrane to reach the cytosol is far from being molecularly described. Previous studies have suggested that the *B. anthracis* toxins, the lethal toxin (PA63 and LF) and the edema toxin (PA63 and EF), belong to the group of the A−B type toxin (whose prototype is diphtheria toxin, DT) regarding the existence of one B moiety (PA63) interacting with either of two A subunits (EF and LF), as well as the nature of the mechanism of internalization (see the introduction). However, from a structural point of view PA63 behaves more like the α-toxin of *Staphylococcus aureus* (a pore-forming toxin; *46*, *47*) than like DT: it has a β-sheet structure (*48*) and the membrane competent structure is a heptamer (*22*). The structure of the detergent-bound heptameric form of α-toxin has been recently determined at 1.9 Å resolution by X-ray diffraction (*49*). The α-toxin oligomer has a mushroom shape in which the stem domain is a 14-strand antiparallel β-barrel which crosses the cell membrane and creates a water-filled channel. Each monomer contributes to the barrel structure by insertion in the lipid membrane of a pair of β-strands. According to the crystal structure of the PA63 oligomer, a similar structure could characterize the insertion of PA63 in a lipid membrane. Our FTIR data support the hypothesis of the membrane interaction being mediated by the formation of β-sheets characterized by the presence of intersheets hydrogen bonds. Indeed, in the presence of the lipid membrane, the frequency of absorption

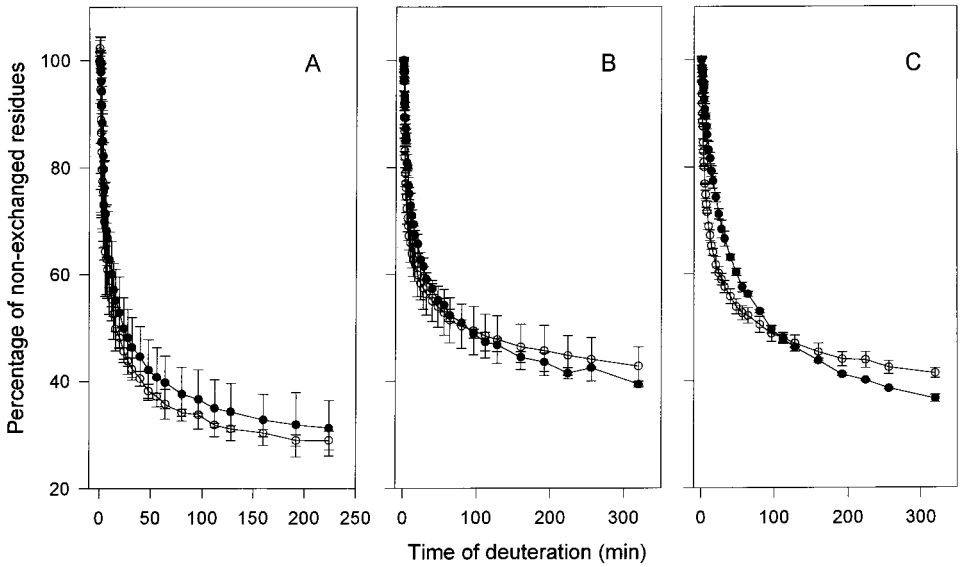

FIGURE 5: Evolution of the proportion of non-exchanged residues as a function of the deuteration time. (A) PA63 at pH 5.0; (B) EF at pH 7.2; (C) EF at pH 5.0 with (●) and without (○) lipids. Each curve is the average of three experiments, and the error bars represent the standard deviation.

of PA63 is shifted from 1633 to 1623 cm^{-1}. The low-frequency absorption (1623 cm^{-1}) is characteristic of β-strands forming strong hydrogen bonds which may arise from intermolecular bonds between aggregated or oligomerized proteins (*50*). Moreover, the number of residues of PA63 accessible to solvent and therefore able to undergo a hydrogen/deuterium exchange is not strongly modified by the interaction with the lipid membrane, which suggests that only a few number of residues are involved in this interaction, as it would be the case if a monomer would contribute only two β-strands in the membrane. Upon incubation with the lipid membrane, the content of organized structures increased at the expense of the random and the turn structures. This could be the consequence of the packing of the seven monomers at the membrane surface.

One main question that still has to be solved is the mechanism by which PA63 mediates the translocation of EF and LF in the cell cytoplasm. It has been previously demonstrated that PA63 was able to induce a channel formation in planar lipid bilayers (*19*). The crystal structure and our data suggest that this channel may adopt a β-barrel structure. Whether or not this channel could translocate EF and LF in an unfolded form remains to be solved. However, the strong interaction of LF (*17*) and EF with the lipid membrane in the absence of PA63 suggests that they may play an active role in their own translocation by forming a complex with PA63. Contrary to PA63 which is mostly a β-sheet protein, LF (*17*) and EF have a high helical content (39%). Their binding to the lipid membrane is characterized by (i) an increase of the helical content (with a decrease of the random structure), (ii) a shift of the β-sheet component to a IR lower wavelength, and (iii) a hydrogen/deuterium exchange almost identical to the exchange observed in the absence of lipids. This is very similar to the modifications observed upon binding of PA63 to the lipid vesicles, suggesting that the three proteins may adopt similar strategies, such as an oligomeric form, to interact with the lipid membrane. The hypothesis of LF and EF oligomerization is in agreement with previous fluorescence studies which demonstrated that the Trp fluorescence of these proteins was quenched when the proteins were inserted in the lipid membrane (*18*). The presence of an identical low-frequency component (1623 cm^{-1}) in the IR spectra of the three proteins of toxins of *B. anthracis* when incubated in the presence of a lipid membrane suggests that they might be able to form a heterostructure in the lipid membrane: a β-barrel that would be formed by the seven (or fewer) monomers of PA63 and by a still unknown number of monomers of either LF or EF. The active "translocation machinery" would then be a heterocomplex formed by the association of β-strands from PA63 and one of the two A subunits (LF or EF).

The data given in this paper are providing new and important insights into the mechanism of translocation of EF and LF across the lipid membrane. As described and characterized by other authors, the first three steps of intoxication of the *B. anthracis* toxins are (i) the binding of PA to specific cell receptors, (ii) the cleavage of PA and the binding of either LF or EF to PA63, and (iii) the endocytosis of the complex. Once in the endosomal pathway, the complex meets a low pH that allows the insertion of PA63 into the membrane. One striking difference is however observed between LF and EF: the interaction of LF with the lipid membrane is strictly dependent upon low pH whereas that of EF is not pH-dependent. Whether or not EF may first insert in the lipid membrane remains unclear, but it seems that its translocation requires the presence of PA63 in the lipid membrane. As previously demonstrated, the interaction of LF with the lipid membrane is reversible when the pH is brought back to neutral (*17*). After translocation, LF is therefore most probably released in the cytoplasm where it will exert its lethal activity, whereas PA63 remains in the lipid membrane. Since EF strongly interacts with the lipid membrane at pH 7.2, it may not be completely released in the cell cytoplasm. The only requirement for activity is to expose to the cytosol the catalytic domains, and this does not exclude the presence of transmembrane regions: most adenylate cyclases are membrane proteins characterized by one or more transmembrane domains (*51*). The analysis of the CYA mutants has shown that the region(s) responsible for the interaction at pH 7.2 is (are) localized on the protein domain which carries the nucleotide and the calmodulin binding sites (CYA62) which could

suggest that, even though EF is a secreted protein, it may adopt, in the endosomal membrane, a topological organization similar to other adenylate cyclases.

ACKNOWLEDGMENT

We thank K. Oberg and C. Guidi-Rontani for helpful discussions.

REFERENCES

1. Leppla, S. H. (1991) in *Sourcebook of Bacterial Protein Toxins* (Alouf, J. E., and Freer, J. H., Ed.) pp 277−302, Academic Press, London.
2. Smith, H., and Stanley, J. L. (1962) *J. Gen. Microbiol. 29*, 517−521.
3. Harris-Smith, P. W., Smith, H., and Keppie, J. (1958) *J. Gen. Microbiol. 19*, 91−103.
4. Escuyer, V., and Collier, R. J. (1991) *Infect. Immun. 59*, 3381−3386.
5. Singh, Y., Chaudhary, V. K., and Leppla, S. H. (1989) *J. Biol. Chem. 264*, 19103−19107.
6. Klimpel, K. R., Molloy, S. S., Thomas, G., and Leppla, S. H. (1992) *Proc. Natl. Acad. Sci. U.S.A. 89*, 10277−10281.
7. Molloy, S. S., Bresnahan, P. A., Leppla, S. H., Klimpel, K. R., and Thomas, G. (1992) *J. Biol. Chem. 267*, 16396−16402.
8. Leppla, S. H., Friedlander, A. M., and Cora, E. M. (1988) in *Bacterial Protein Toxins* (Fehrenbach, F., Alouf, J. E., Falmagne, P., Goebel, W., Jeljaszewicz, J., Jurgen, D., and Rappuoli, R., Eds.) pp 111−112, Gustav Fischer, New York.
9. Draper, R. K., and Simon, M. I. (1980) *J. Cell. Biol. 87*, 849−854.
10. Sandvig, K., and Olsnes, S. (1980) *J. Cell. Biol. 87*, 828−832.
11. Gordon, V. M., Leppla, S. H., and Hewlett, E. L. (1988) *Infect. Immun. 56*, 1066−1069.
12. Friedlander, A. M. (1986) *J. Biol. Chem. 261*, 7123−7126.
13. Leppla, S. H. (1982) *Proc. Natl. Acad. Sci. U.S.A. 79*, 3162−3166.
14. Leppla, S. H. (1984) *Adv. Cyclic Nucleotide Protein Phosphorylation Res. 17*, 189−198.
15. Labruyère, E., Mock, M., Ladant, D., Michelson, S., Gilles, A. M., Laoide, B., and Bârzu, O. (1990) *Biochemistry 29*, 4922−4928.
16. Klimpel, K. R., Arora, N., and Leppla, S. H. (1994) *Mol. Microbiol. 13*, 1093−1100.
17. Wang, X. M., Mock, M., Ruysschaert, J. M., and Cabiaux, V. (1996) *Biochemistry 35*, 14939−14946.
18. Kochi, S. K., Martin, I., Schiavo, G., Mock, M., and Cabiaux, V. (1994) *Biochemistry 33*, 2604−2609.
19. Blaustein, R. O., Koehler, T. M., Collier, R. J., and Finkelstein, A. (1989) *Proc. Natl. Acad. Sci. U.S.A. 86*, 2209−2213.
20. Koehler, T. M., and Collier, R. J. (1991) *Mol. Microbiol. 5*, 1501−1506.
21. Milne, J. C., and Collier, R. J. (1993) *Mol. Microbiol. 10*, 647−653.
22. Milne, J. C., Furlong, D., Hanna, P. C., Wall, J. S., and Collier, R. J. (1994) *J. Biol. Chem. 269*, 20607−20612.
23. Kagawa, Y., and Racker, E. (1971) *J. Biol. Chem. 246*, 5477−5487.
24. Pezard, C., Duflot, E., and Mock, M. (1993) *J. Gen. Microbiol. 139*, 2459−2463.
25. Laemmli, U. K. (1970) *Nature 227*, 680−685.
26. Matsudaira, P. (1987) *J. Biol. Chem. 246*, 10035−10040.
27. Brune, D. C. (1992) *Anal. Biochem. 207*, 285−290.
28. Hope, M. J., Bally, M. B., Webb, G., and Cullis, P. R. (1985) *Biochim. Biophys. Acta 812*, 55−65.
29. Mrsny, R. J., Volwerk, J. J., and Griffith, O. H. (1986) *Chem. Phys. Lipids 39*, 185−191.
30. Goormaghtigh, E., Vigneron, L., Scarborough, G. A., and Ruysschaert, J. M. (1994) *J. Biol. Chem. 269*, 27409−27413.
31. Fringeli, U. P., and Günthard, H. H. (1981) *Mol. Biol. Biochem. Biophys. 31*, 270−332.
32. Goormaghtigh, E., and Ruysschaert, J. M. (1990) in *Molecular Description of Biological Components by Computer Aided Conformational Analysis* (Brasseur, R., Ed.) pp 285−329, CRC Press, Boca Raton, FL.
33. Rothschild, K. J., and Clark, N. (1982) *Methods Enzymol. 88*, 696−714.
34. Cortijo, M., Alonso, A., Gomez-Fernandez, J. C., and Chapman, D. (1982) *J. Mol. Biol. 157*, 597−618.
35. Goormaghtigh, E., Cabiaux, V., and Ruysschaert, J. M. (1990) *Eur. J. Biochem. 193*, 409−420.
36. Goormaghtigh, E., Cabiaux, V., and Ruysschaert, J. M. (1994) *Subcell Biochem. 23*, 329−450.
37. Cabiaux, V., Brasseur, R., Wattiez, R., Falmagne, P., Ruysschaert, J. M., and Goormaghtigh, E. (1989) *J. Biol. Chem. 264*, 4928−4938.
38. de Jongh, H. H. J., Goormaghtigh, E., and Ruysschaert, J. M. (1995) *Biochemistry 34*, 172−179.
39. Raussens, V., Narayanaswami, V., Goormaghtigh, E., Ryan, R. O., and Ruysschaert, J. M. (1996) *J. Biol. Chem. 271*, 23089−23095.
40. Challou, N., Goormaghtigh, E., Cabiaux, V., Conrath, K., and Ruysschaert, J. M. (1994) *Biochemistry 33*, 6902−6910.
41. Goormaghtigh, E., Brasseur, R., Huart, P., and Ruysschaert, J. M. (1987) *Biochemistry 26*, 1789−1794.
42. Goormaghtigh, E., De Meutter, J., Cabiaux, V., Szoka, F., and Ruysschaert, J. M. (1990) *Eur. J. Biochem. 195*, 421−429.
43. Goormaghtigh, E., Cabiaux, V., De Meutter, J., Rosseneu, M. Y., and Ruysschaert, J. M. (1993) *Biochemistry 32*, 6104−6110.
44. Sonveaux, N., Conrath, K., Capiau, C., Brasseur, R., Goormaghtigh, E., and Ruysschaert, J. M. (1994) *J. Biol. Chem. 269*, 25637−25645.
45. Vandenbussche, G., Clercx, A., Clercx, M., Curstedt, T., Johansson, J., Jörnvall, H., and Ruysschaert, J. M. (1992) *Biochemistry 31*, 9169−9176.
46. Valeva, A., Weisser, A., Walker, B., Kehoe, M., Bayley, H., Bhakdi, S., and Palmer, M. (1996) *EMBO J. 15*, 1857−1864.
47. Gouaux, J. E., Braha, O., Hobaugh, M. R., Song, L., Cheley, S., Shustak, C., and Bayley, H. (1994) *Proc. Natl. Acad. Sci. U.S.A. 91*, 12828−12831.
48. Petosa, C., Collier, R. J., Klimpel, K. R., Leppla, S. H., and Liddington, R. C. (1997) *Nature 385*, 833−838.
49. Song, L., Hobaugh, M. R., Shustak, C., Cheley, S., Bayley, H. and Gouaux, J. E. (1996) *Science 274*, 1859−1866.
50. Jackson, M., and Mantsch, H. H. (1995) *Crit. Rev. Biochem. Mol. Biol. 30*, 95−120.
51. Tang, W. J., and Gilman, A. G. (1992) *Cell 70*, 869−872.

BI971661K